

Carbon nanotubes introduced into the abdominal cavity of mice show asbestos-like pathogenicity in a pilot study

CRAIG A. POLAND¹, RODGER DUFFIN¹, IAN KINLOCH², ANDREW MAYNARD³, WILLIAM A. H. WALLACE¹, ANTHONY SEATON⁴, VICKI STONE⁵, SIMON BROWN¹, WILLIAM MACNEE¹ AND KEN DONALDSON^{1*}

¹MRC/University of Edinburgh, Centre for Inflammation Research, Queen's Medical Research Institute, 47 Little France Crescent, Edinburgh EH16 4TJ, UK

²School of Materials, University of Manchester, Grosvenor Street, Manchester M1 7HS, UK

³Woodrow Wilson International Center for Scholars, 1300 Pennsylvania Avenue, NW, Washington DC 20004-3027, USA

⁴Institute of Occupational Medicine, Research Avenue North, Riccarton, Edinburgh EH14 4AP, UK

⁵School of Life Sciences, Napier University, Colinton Road, Edinburgh EH10 5DT, UK

*e-mail: ken.donaldson@ed.ac.uk

Published online: 20 May 2008; doi:10.1038/nnano.2008.111

Carbon nanotubes¹ have distinctive characteristics², but their needle-like fibre shape has been compared to asbestos³, raising concerns that widespread use of carbon nanotubes may lead to mesothelioma, cancer of the lining of the lungs caused by exposure to asbestos⁴. Here we show that exposing the mesothelial lining of the body cavity of mice, as a surrogate for the mesothelial lining of the chest cavity, to long multiwalled carbon nanotubes results in asbestos-like, length-dependent, pathogenic behaviour. This includes inflammation and the formation of lesions known as granulomas. This is of considerable importance, because research and business communities continue to invest heavily in carbon nanotubes for a wide range of products⁵ under the assumption that they are no more hazardous than graphite. Our results suggest the need for further research and great caution before introducing such products into the market if long-term harm is to be avoided.

Carbon nanotubes (CNTs) are often considered to epitomize the field of nanotechnology—a diverse collection of nanoscale technologies that are projected to be associated with \$2.6 trillion worth of manufactured goods by the year 2014 (ref. 6). The global market for CNTs is predicted to grow to between \$1 billion and \$2 billion by 2014, spurred on by new and increasing industrial demands⁵. Meanwhile, widespread concerns have been raised that a poor understanding of how to safely develop and use engineered nanomaterials—including carbon nanotubes—could undermine business interests and unduly jeopardize human health and the environment⁷.

The unique nanometre-scale structure of CNTs is based on a graphene cylinder, typically a few nanometres in diameter, which can range in length from a few micrometres to millimetres³. Single-walled nanotubes (SWNTs) consist of one such cylinder, and multiwalled nanotubes (MWNTs), as used in this study, comprise 2 to 50 such cylinders concentrically stacked with a common long axis. This structure gives nanotubes an unusual

combination of properties that are highly desirable in many industrial products^{3,8}. Their high aspect ratio (ratio of length and width) makes them an attractive structural material, but their nanometre-scale diameter and needle-like shape have drawn comparisons with asbestos^{9,10}.

Exposure during mining and the industrial use of asbestos led to a global pandemic of lung diseases. Study of disease in exposed populations showed that the main body of the lung was a target for asbestos fibres, resulting in both lung cancer and scarring of the lungs (asbestosis). The outside surface lining of the lung and its associated tissue, the pleura, was found also to be a target, with cancer of the pleura (mesothelioma), fluid accumulation in the pleural space (effusion) and scarring of the pleura (pleural thickening and plaque formation) being found in association with asbestos exposure¹¹. A critical factor underlying this pandemic is a prolonged latency period between exposure and the development of mesothelioma, the hallmark cancer of asbestos exposure. Toxicologists have derived a paradigm in which a hazardous fibre is one that is thinner than 3 μm , longer than $\sim 20 \mu\text{m}$ and biopersistent in the lungs, in other words not dissolving or breaking into shorter fibres¹². Above all, for there to be any adverse effect, the numbers of such fibres must reach a sufficient level to cause chronic activation of inflammatory cells, genotoxicity, fibrosis and cancer in the target tissue^{11,13}.

A superficial resemblance between nanomaterials such as CNTs and asbestos has led scientists to challenge the research community to 'Assess whether fibre-shaped nanoparticles present a unique health risk'¹⁴. Published studies have evaluated acute responses to CNTs in cell cultures and the lungs of animal models^{10,15–17}, but the hypothesis that CNTs can behave like asbestos at the mesothelium has not previously been tested. The mesothelial layer is the cell layer that covers the internal surfaces of the pleural (chest) and peritoneal (abdominal) cavities and the exterior surfaces of the organs they contain, lubricating their motion. When cancer occurs in the mesothelium, as is the case

Table 1 Characterization of multiwalled carbon nanotubes.

	NT _{tang1}	NT _{tang2}	NT _{long1}	NT _{long2}
Source	NanoLab, Inc.	NanoLab, Inc.	Mitsui & Co.	Dr Ian Kinloch (University of Manchester)
Description of morphology (from SEM, TEM and light microscopy)	Short MWNTs forming tightly packed spherical agglomerates, a large proportion of which are in the respirable size range <5 µm, with frayed edges of singlet nanotubes.	Bundles of intermediate-length MWNTs. Often stellate in form with longer fibres protruding from the central tangled agglomerate, a large proportion of which are in respirable size range <5 µm.	Dispersed bundles and singlets of long and intermediate-length MWNTs, many in the range 10–20 µm and longer. Many very short fibres often decorate the long fibres.	Regular bundles and ropes of MWNTs with a fairly constant length and diameter. Typically, single ropes of tubes are more than 20 µm in length.
Diameter as supplied by the manufacturer (nm, mean ± s.e.m.)	15 ± 5	15 ± 5	40–50	20–100
Diameter as determined by authors (nm, mean ± s.e.m.)	14.84 ± 0.50	10.40 ± 0.32	84.89 ± 1.9	165.02 ± 4.68
Length as supplied by the manufacturer (µm)	1–5	5–20	Mean 13	Max 56
Percentage fibres greater than 15 µm (see Supplementary Information, Methods, for methodology)	‡	‡	24.04	84.26
Percentage fibres greater than 20 µm (see Supplementary Information, Methods, for methodology)	‡	‡	11.54	76.85
Endotoxin (pg ml ⁻¹)*	ND	ND	ND	ND
Soluble metals (µg g ⁻¹) [†] (see Supplementary Information, Fig. S2, for a full analysis)				
Fe	7.9	13.4	ND [‡]	37.3
Cu	5.1	1	1.2	1.2
V	ND [‡]	ND [‡]	0.8	ND
Ni	9.7	5	6.2	6.2
Zn	5.5	7.5	0.7	ND [‡]
Co	3.7	ND [‡]	1.9	3.4

ND = not detectable.

*Endotoxin detection limit <10 pg ml⁻¹.†Metal analysis detection limit <0.1 µg g⁻¹.

‡The presence of long fibres could not be reliably determined.

in a proportion of individuals exposed to asbestos, the cancer is termed mesothelioma¹¹. Mesothelioma is almost exclusively found following asbestos exposure and mesothelioma is a particle response unique to fibre-shaped particles¹⁸.

We previously recorded that direct exposure of the mesothelium by intraperitoneal (i.p.) injection of long amosite asbestos fibres resulted in an exaggerated inflammatory response, but there was little or no response to injected short amosite fibres¹⁹. This most likely reflects the extreme sensitivity of the mesothelium to long fibres^{20,21}. We therefore hypothesize that the most important acute response to long CNTs, if they were to behave like asbestos, would be mesothelial injury.

Amosite, or brown asbestos, is an amphibole form of asbestos and the samples used here were prepared for pathology studies undertaken to investigate the role of fibre length²². The long-fibre amosite (LFA) used in this study was South African amosite, which was prepared to have a large proportion of long fibres, and the short-fibre amosite (SFA) sample was prepared from the long-fibre sample by comminution in a ball mill²². In the present study LFA and SFA were used as positive and negative controls, respectively^{19,22}. The four samples of MWNTs were chosen to assess the role of long rigid fibres in stimulating a mesothelial response similar to that caused by LFA. Two of the MWNT samples, NT_{long1} and NT_{long2}, contained a substantial proportion of long straight fibres longer than 20 µm, and the other two samples, NT_{tang1} and NT_{tang2}, consisted of CNTs arranged in low-aspect-ratio tangled aggregates. Full characterization of the MWNT samples and the

derivation of these classifications are provided in Table 1. In addition, a nanoparticulate carbon black (NPCB) sample was used as a non-fibrous graphene control. Transmission electron microscopy (TEM) and optical analysis of NT_{long2} samples confirmed that the nanotube fibres were not all single tubes, but rather were ‘wires’ or ‘ropes’ of intertwined single CNTs, rendering them visible by light microscopy in the tissue and cell samples.

Each material was injected in a 50 µg dose into the peritoneal (abdominal) cavity of mice and the cavity systematically washed out at 24 h or 7 days post exposure with physiological saline, in a process termed lavage, to provide a lavageate that contained the cells and molecules present in the peritoneal cavity. The response was assessed by measuring protein levels and cell populations in the lavageate of the peritoneal cavity 24 h later¹⁹. The pathogenic response to long fibres is typified by an alteration in the normal structure of the mesothelial surface to produce a scar-like structure (lesion) called a granuloma. Histological quantification of granulomas on the peritoneal side of the diaphragm²¹ and foreign body giant cells (FBGCs) was carried out after 7 days.

The normal inflammatory response to pathogenic particles or their soluble components is inflammation, with polymorphonuclear leukocyte (PMN) and protein exudation. Only the samples that contained long fibres (LFA, NT_{long1} and NT_{long2}) caused significant PMN (Fig. 1a) or protein (Fig. 1b) exudation. FBGCs (Fig. 1c) and granulomas on the peritoneal side of the diaphragm (Fig. 1d; see also Fig. 2b,c and Supplementary Information, Tables S1 and S2) were also seen with the

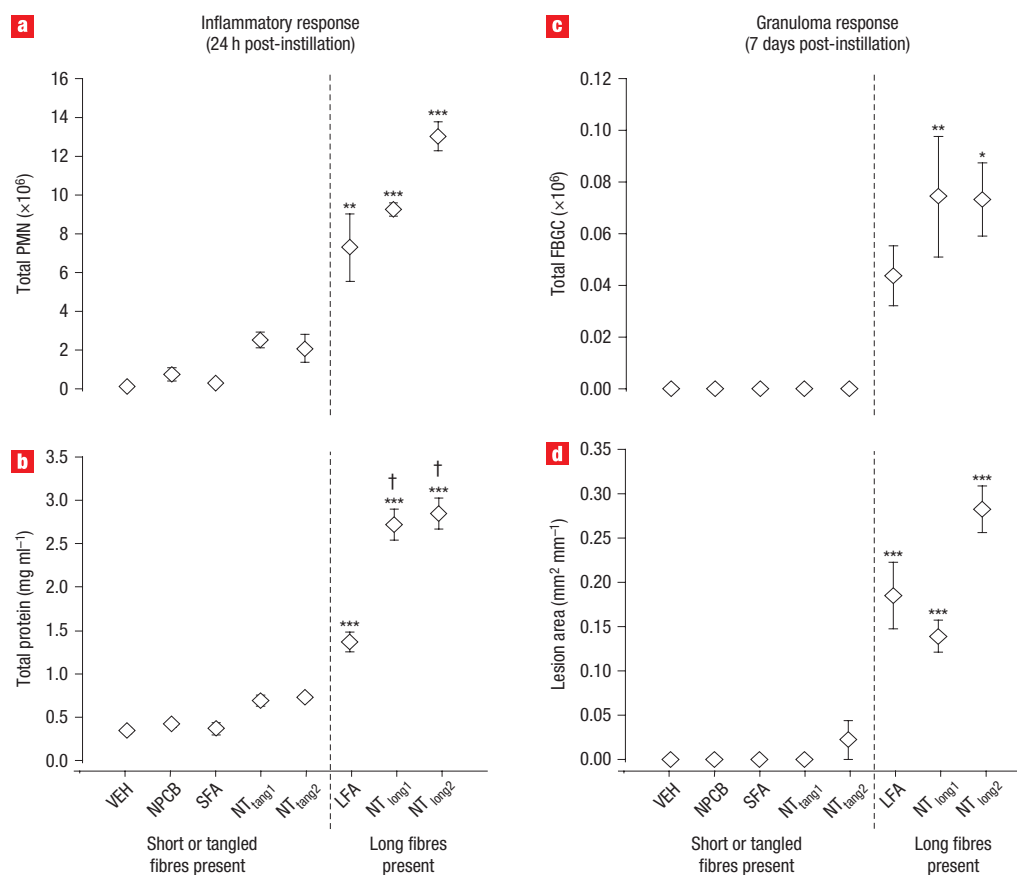


Figure 1 Recruitment of inflammatory cells in the peritoneal cavity after introduction of fibres. Female C57Bl/6 mice were intraperitoneally instilled with 50 μg of vehicle control (VEH, 0.5% BSA/saline; 0.5 ml), nanoparticulate carbon black (NPCB), short-fibre amosite (SFA), long-fibre amosite (LFA), two curled/tangled MWNT samples of different lengths (NT_{tang1}, NT_{tang2}) and two samples containing long MWNTs (NT_{long1}, NT_{long2}). After 24 h and 7 days post-exposure, the mice were killed and the peritoneal cavity lavaged. **a,b**, At 24 h, inflammatory response was evaluated using differential cell counts to establish total PMN population (**a**, mean \pm s.e.m.; VEH, $n = 3$; NPCB, $n = 3$; SFA, $n = 3$; NT_{tang1}, $n = 3$; NT_{tang2}, $n = 4$; LFA, $n = 6$; NT_{long1}, $n = 4$; NT_{long2}, $n = 3$), and total protein (**b**, mean \pm s.e.m.; VEH, $n = 5$; NPCB, $n = 4$; SFA, $n = 3$; NT_{tang1}, $n = 6$; NT_{tang2}, $n = 6$; LFA, $n = 6$; NT_{long1}, $n = 8$; NT_{long2}, $n = 6$). **c**, At 7 days, granuloma response was investigated by measuring the total foreign body giant cell (FBGC) population (mean \pm s.e.m.; VEH, $n = 6$; NPCB, $n = 4$; SFA, $n = 5$; NT_{tang1}, $n = 4$; NT_{tang2}, $n = 4$; LFA, $n = 4$; NT_{long1}, $n = 6$; NT_{long2}, $n = 5$), which marks the chronic foreign-body-induced inflammation. **d**, Histological sections of excised diaphragms show the extent of granuloma formation at the peritoneal surface of the diaphragm (mean \pm s.e.m.; $n = 3$). The nonsignificant increase in granuloma shown in mice treated with NT_{tang2} is a consequence of a small granuloma response in a single mouse (see Supplementary Information for details of the methodology and outcome of this part of the study). * $P < 0.05$, ** $P < 0.01$, *** $P < 0.001$ versus vehicle control; † $P < 0.001$ versus LFA.

long-fibre-containing samples. This foreign body response is the normal reaction to indigestible or non-degradable material that macrophages cannot eliminate. The granulomas comprised aggregates of cells containing fibres, most likely macrophages, and also FBGCs, with MWNT/asbestos fibres and associated deposition of collagen within the lesions (Fig. 2b,c). The mesothelial lining on the pleural side of the diaphragm was normal in every case. The PMN inflammation had decreased by 7 days, as the focus of inflammation changed from the peritoneal cavity in general to the granulomas (data not shown). In contrast, particle samples that did not contain detectable long fibres (although they may have contained low-level contamination with long fibres)—NPCB, SFA, NT_{tang1} and NT_{tang2}—failed to cause any significant inflammation at 1 day or giant cell formation at 7 days. A small nonsignificant granuloma response in one of three of the NT_{tang2}-treated mice (see Fig. 1d; see also Supplementary Information, Table S1 and Fig. S3) could have been a consequence of a contamination of long fibres that was so low that they were not detected in the fibre size analysis.

Alternatively, this low-level response could have been caused by some other unidentified component of the NT_{tang2}, or the granulomas could have arisen spontaneously by chance. Although statistical analysis indicated a clear lack of effect from the short MWNT samples, a similar study in a larger group of animals would provide greater confidence in these differences. Neither soluble metals nor endotoxin contamination of long samples were correlated with the greater inflammogenicity and granuloma formation seen with the NT_{long} samples (see Table 1).

To further examine the role of water-soluble components, these were collected from a 50- μg dose of NT_{long1} and NT_{long2} by overnight mixing in 0.5% bovine serum albumin (BSA)/sterile saline vehicle. The soluble components produced no significant inflammatory effects 24 h after injection into the mouse peritoneal cavity (see Supplementary Information, Fig. S2). Neither can levels of total metals explain the differences between short and long responses seen with nanotube samples (see Supplementary Information, Fig. S1). Transition metals have

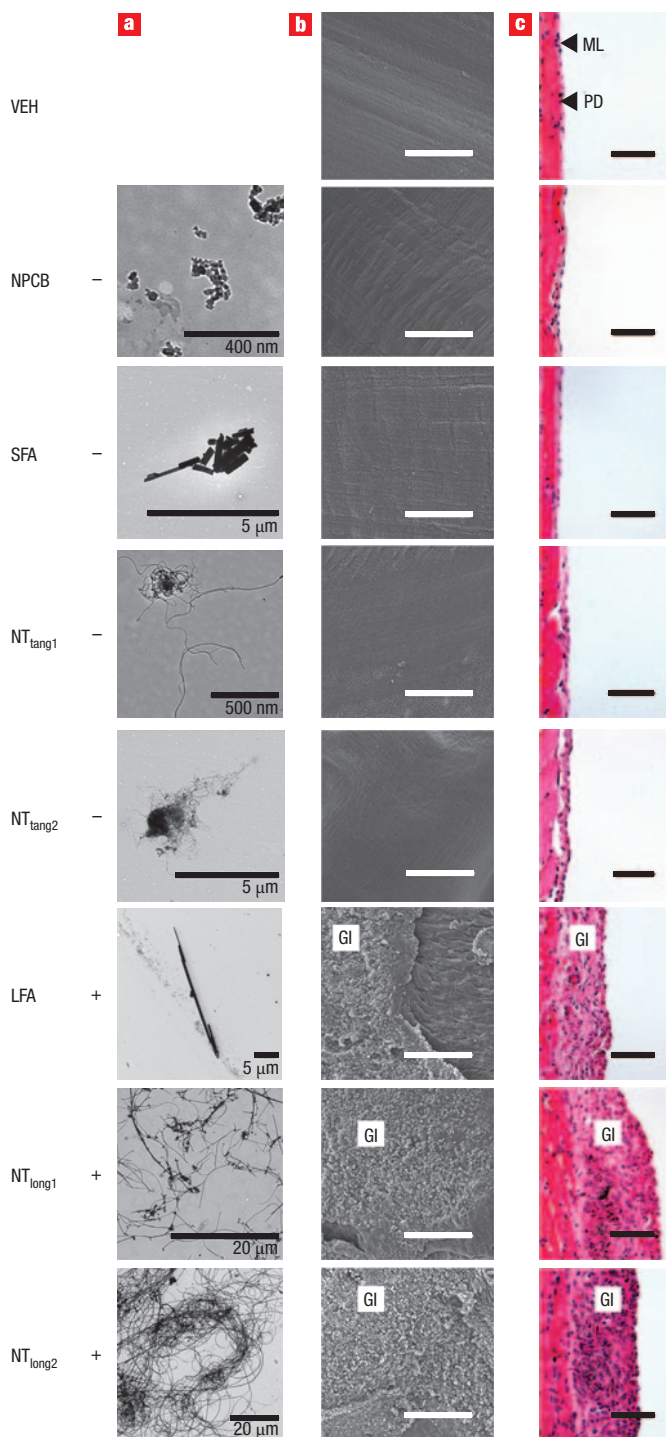


Figure 2 Effect of the particle/fibre on diaphragms after 7 days. **a**, TEM images show the presence (+) or absence (–) of long fibres in the samples used. Female C57Bl/6 mice were injected i.p. with 50 μg of sample, killed after 7 days, and the diaphragms excised and prepared for visualization. **b,c**, SEM images (**b**) and haematoxylin and eosin histology sections ($n = 3$) (**c**) of the diaphragms show the presence of granulomatous inflammation (Gl) in mice exposed to LFA, $\text{NT}_{\text{long}1}$ and $\text{NT}_{\text{long}2}$. A small granuloma response in one of the three mice treated with $\text{NT}_{\text{tang}2}$ (see Supplementary Information, Tables S1 and S2, for raw data and statistical analysis) was observed. The muscular portion of the peritoneal diaphragm (PD) and the mesothelial layer (ML) are aligned to show granulomatous inflammation at the peritoneal aspect of the diaphragm surface. Scale bars in **b**: 200 μm . Scale bars in **c**: 50 μm .

been implicated in CNT-mediated stress in an earlier published study on nanotubes *in vitro*²³, but neither soluble nor total metals can explain the differences in peritoneal response seen here with long and short MWNTs. There is a remote possibility that some unmeasured metal or other component could contribute to this difference but, in the opinion of the authors, it is unlikely. Although our data show that short CNTs do not mimic the behaviour of long asbestos, our data cannot preclude the possibility that short CNTs are harmful by conformation to some other paradigm that was not addressed here, such as intrinsic toxicity as particles, as opposed to fibres.

In attempting to phagocytose or engulf a fibre longer than the length they can completely enclose, the specialized ‘engulfing cells’, macrophages, are chronically stimulated to release mediators that cause inflammation^{24,25}. In this inflammatory milieu the conditions, including the cytokine environment, that encourage macrophage fusion are produced, leading to giant cell formation (Fig. 3c,f). The macrophages that are undergoing frustrated phagocytosis are not necessarily the ones that form giant cells, as shown by the fact that macrophages are stimulated to undergo formation into giant cells *in vitro* with a combination of cytokines alone²⁶. So, although we have no quantitative data on the role of frustrated phagocytosis, images from the lavage of animals exposed to LFA and long MWNTs (Fig. 3a,d) show that frustrated phagocytosis did occur. No FBGCs were found in the lavage of animals exposed to NPCB, SFA, nor the short, tangled MWNT samples, and complete phagocytosis was evident in macrophages from the lavage (see Fig. 3b,e for SFA and $\text{NT}_{\text{tang}1}$, respectively).

Our aim was to investigate commercial samples of CNTs to obtain real-world relevance and compare pathogenicity and we showed clear differences between long and short/tangled MWNTs. However, there was an attendant problem in that there are differences in the source, preparation and purification of different commercial CNTs and therefore potential differences in physicochemistry and contaminating metals. For example, the two short tangled samples were acid-treated and this may have resulted in alterations. We have addressed this here and largely discounted factors other than length, but another strategy to critically address the role of length is to mill long CNTs and compare the unmilled (long) with the milled (short) fibres, so minimizing differences except for length. Short CNTs may be pathogenic by virtue of being particles, and that would not have been detected in the assays used here, which are sensitive only to asbestos/fibre-type effects.

The discrimination in terms of asbestos-like hazard between short/tangled and long MWNTs shown after low-dose injection of fibres in our study emphasizes the importance of choosing the correct assay. In this case the assay was based on the uniqueness of the mesothelial response to long fibres. We observed that long MWNTs produced inflammation, FBGCs and granulomas that were qualitatively and quantitatively similar to the foreign body inflammatory response caused by long asbestos. In contrast, NPCB did not cause peritoneal inflammation, highlighting the fact that fibrous shape dominates over simple graphene chemistry in effects on the mesothelium.

The fact that CNTs can be produced in a morphology that implies an asbestos-like hazard, although unwelcome, was predicted on the basis of the fibre paradigm^{4,12}. The single published study on CNTs in workplace air²⁷ found that airborne particles that resemble the tangled MWNT samples shown here have low potency. We note that two of the three commercially obtained samples of MWNTs used here ($\text{NT}_{\text{tang}1}$ and $\text{NT}_{\text{tang}2}$) had similar short/tangled morphologies due to their curled/tangled structure. This morphology showed little potency in the assays and so these would not be predicted to behave like asbestos.

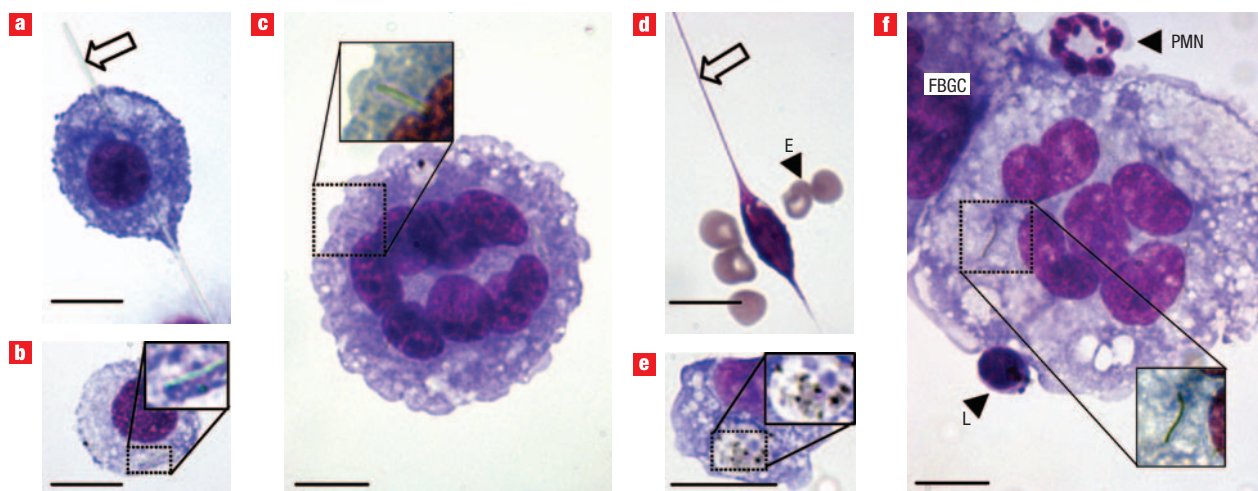


Figure 3 Effect of fibre length on phagocytosis by peritoneal macrophages. **a,b**, Histological sections show incorporation of LFA (**a**, arrow) leading to ‘frustrated phagocytosis’, but SFA (**b**, see inset) is successfully phagocytosed. **c**, Representative image of an FBGC after injection of LFA containing short fragments of fibre (see inset). **d**, Like LFA, $NT_{\text{long}2}$ also leads to frustrated phagocytosis (E—erythrocytes). **e**, In contrast, $NT_{\text{tang}1}$ can be readily phagocytosed (see inset). **f**, FBGC is also present after injection of $NT_{\text{long}2}$ (see inset for internalized fibres) (PMN, polymorphonuclear leukocyte; L, lymphocyte). All images are shown at $\times 1,000$ magnification with a $5\ \mu\text{m}$ scale bar.

Our data demonstrate that asbestos-like pathogenic behaviour associated with CNTs conforms to a structure–activity relationship based on length, to which asbestos and other pathogenic fibres conform. Exposure of the mesothelium, however, is based upon the caveat that all materials tested shared a high level of biopersistence, allowing sufficient time for migration through the lung to the mesothelium. As such, our study does not address whether CNTs would be able to reach the mesothelium in sufficient numbers to cause mesothelioma following inhalation exposure. Although the study suggests a potential link between inhalation exposure to long CNTs and mesothelioma, it remains unknown whether there will be sufficient exposure to such particles in the workplace or the environment to reach a threshold dose in the mesothelium. Intraperitoneal injection of long asbestos into the peritoneal cavity of rodents has been demonstrated to cause mesothelioma in the long term²². However, our study did not address whether the mice exposed to long CNTs that developed inflammatory and granulomatous changes would go on to develop mesotheliomas. Neither did our study rule out the possibility that short CNTs may have some intrinsic pathogenicity by virtue of their particulate nature, which would not have been detected in the assays used here, which are specific for fibre effects. These are research questions that must be addressed with some urgency before the commercial use of long CNTs becomes widespread.

METHODS

A panel of four different samples of MWNTs and three different control particles (LFA, SFA and NPCB) was used. The MWNT panel comprised three commercially available nanotubes and one sample produced in an academic research laboratory. The nanotube samples used were a sample of long MWNTs ($NT_{\text{long}1}$; Mitsui & Co.), a second MWNT sample of largely long fibres ($NT_{\text{long}2}$; University of Manchester), and two curled/tangled NT samples either cut (using a proprietary process) to form predominantly short fibres ($NT_{\text{tang}1}$) or with their original length ($NT_{\text{tang}2}$) (NanoLab). The NPCB used was Printex 90 (Degussa). The classification of samples into NT_{long} or NT_{tang} was established from the physical characteristics observed using scanning electron microscopy (SEM), TEM and light microscopy (only TEM images are shown), where appropriate,

to fully describe each sample (Table 1). The diameter of both individual fibres and (in the case of $NT_{\text{tang}1}$ and $NT_{\text{tang}2}$) agglomerate size as well as a length size distribution analysis of the fibres and particles were established. In keeping with World Health Organization (WHO) guidelines²⁸ we counted as a fibre only those particles with an aspect ratio greater than 3:1 and a length $> 5\ \mu\text{m}$.

Inductively coupled plasma mass spectrometry (ICP-MS) analysis was used to quantify contaminating metals (Table 1; see Supplementary Information, Fig. S1 for a full metals analysis), and the presence of bacterial contamination of the particle panel was established by measuring endotoxin levels (Table 1). Samples were prepared for *in vivo* use by ultrasonication in a sterile 0.5% BSA/saline solution and were administered by injection into the peritoneal cavity of female C57Bl/6 mice (aged 8 weeks) at a dose of $100\ \mu\text{g}\ \text{ml}^{-1}$ (0.5 ml; total dose $50\ \mu\text{g}$ per mouse). After 24 h and 7 days the mice were killed by cervical dislocation and the peritoneal cavity lavaged using three 2 ml washes of ice-cold sterile saline, which were pooled together on ice. The 24-h timepoint was chosen based on our experience from previous studies, which indicated that at this timepoint we would be able to discriminate between different particles in their ability to cause inflammation. The 7-day timepoint was chosen to allow time for fibrosis to develop in the granulomas at the diaphragm. The lavage fluid was centrifuged to separate the cellular fraction, and the supernatant protein content was established using a BCA protein assay (VEH, $n = 5$; NPCB, $n = 4$; SFA, $n = 3$; $NT_{\text{tang}1}$, $n = 6$; $NT_{\text{tang}2}$, $n = 6$; LFA, $n = 6$; $NT_{\text{long}1}$, $n = 8$; $NT_{\text{long}2}$, $n = 6$). Cyto-centrifugation preparations were made using the isolated cells, and differential cell counts were performed to establish leukocyte populations (VEH, $n = 3$; NPCB, $n = 3$; SFA, $n = 3$; $NT_{\text{tang}1}$, $n = 3$; $NT_{\text{tang}2}$, $n = 4$; LFA, $n = 6$; $NT_{\text{long}1}$, $n = 4$; $NT_{\text{long}2}$, $n = 3$). At 7 days the diaphragm was carefully removed from the mice and fixed, sectioned, and haematoxylin and eosin stained for gross pathology (VEH, $n = 4$; NPCB, $n = 3$; SFA, $n = 3$; $NT_{\text{tang}1}$, $n = 3$; $NT_{\text{tang}2}$, $n = 3$; LFA, $n = 3$; $NT_{\text{long}1}$, $n = 4$; $NT_{\text{long}2}$, $n = 3$). The granulomatous lesions present with each section was quantified using serial images taken at $\times 100$ magnification using QCapture Pro software (Media Cybernetics) and the mean lesion area and length of the complete diaphragms (see Supplementary Information, Fig. S3) established using Image-Pro Plus software (Media Cybernetics). Diaphragms removed for surface analysis by SEM were fixed, osmified and gold-sputter-coated for viewing under SEM. All data are expressed as a mean \pm s.e.m. and analysed using one-way analysis of variance (ANOVA). Multiple comparisons were analysed using the Tukey-HSD method and in all cases, values of $P < 0.05$ were considered significant. (See Supplementary Information for a full supplementary methodology.)

Received 3 December 2007; accepted 30 April 2008; published 20 May 2008.

References

- Iijima, S. Helical microtubules of graphite carbon. *Nature* **354**, 56–58 (1991).
- Tasis, D., Tagmatarchis, N., Bianco, A. & Prato, M. Chemistry of carbon nanotubes. *Chem. Rev.* **106**, 1105–1136 (2006).
- Donaldson, K. *et al.* Carbon nanotubes: a review of their properties in relation to pulmonary toxicology and workplace safety. *Toxicol. Sci.* **92**, 5–22 (2006).
- Royal Society and Royal Academy of Engineering. *Nanoscience and nanotechnologies: opportunities and uncertainties* (The Royal Society, London, 2004).
- Thayer, A. M. Carbon nanotubes by the metric ton: Anticipating new commercial applications, producers increase capacity. *Chem. Eng. News* **85**, 29–38 (2007).
- Holman, M. W. & Lackner, D. I. *The Nanotech Report* 4th edn (Lux Research, New York, 2006).
- The risk in nanotechnology: a little risky business. *The Economist* Nov 22 (2007) <http://www.economist.com/displaystory.cfm?story_id=10171212>.
- Maynard, A. D. Nanotechnology: the next big thing, or much ado about nothing? *Ann. Occup. Hyg.* **51**, 1–12 (2007).
- Service, R. F. Nanotoxicology. Nanotechnology grows up. *Science* **304**, 1732–1734 (2004).
- Muller, J. *et al.* Respiratory toxicity of multi-wall carbon nanotubes. *Toxicol. Appl. Pharmacol.* **207**, 221–231 (2005).
- Mossman, B. T. & Churg, A. Mechanisms in the pathogenesis of asbestosis and silicosis. *Am. J. Respir. Crit. Care Med.* **157**, 1666–1680 (1998).
- Donaldson, K. & Tran, C. L. An introduction to the short-term toxicology of respirable industrial fibres. *Mutat. Res.* **553**, 5–9 (2004).
- Kane, A. B. Mechanisms of mineral fibre carcinogenesis, in *Mechanisms of Fibre Carcinogenesis* (ed. Kane, A. B., Boffetta, P., Saracci, R. & Wilbourn, J. D.) 11–34 (IARC, Lyon, 1996).
- Maynard, A. D. *et al.* Safe handling of nanotechnology. *Nature* **444**, 267–269 (2006).
- Warheit, D. B. *et al.* Comparative pulmonary toxicity assessment of single-wall carbon nanotubes in rats. *Toxicol. Sci.* **77**, 117–125 (2004).
- Lam, C. W., James, J. T., McCluskey, R. & Hunter, R. L. Pulmonary toxicity of single-wall carbon nanotubes in mice 7 and 90 days after intratracheal instillation. *Toxicol. Sci.* **77**, 126–134 (2004).
- Shvedova, A. A. *et al.* Unusual inflammatory and fibrogenic pulmonary responses to single-walled carbon nanotubes in mice. *Am. J. Physiol. Lung Cell Mol. Physiol.* **289**, 698–708 (2005).
- Craighead, J. E. *et al.* The pathology of asbestos-associated diseases of the lungs and pleural cavities: diagnostic criteria and proposed grading schema. Report of the Pneumoconiosis Committee of the College of American Pathologists and the National Institute for Occupational Safety and Health. *Arch. Pathol. Lab. Med.* **106**, 544–596 (1982).
- Donaldson, K., Brown, G. M., Brown, D. M., Bolton, R. E. & Davis, J. G. Inflammation generating potential of long and short fiber amosite asbestos samples. *Br. J. Indust. Med.* **46**, 271–276 (1989).
- Lechner, J. F. *et al.* Asbestos-associated chromosomal changes in human mesothelial cells. *Proc. Natl Acad. Sci. USA* **82**, 3884–3888 (1985).
- Moalli, P. A., Macdonald, J. L., Goodglick, L. A. & Kane, A. B. Acute injury and regeneration of the mesothelium in response to asbestos fibers. *Am. J. Pathol.* **128**, 426–445 (1987).
- Davis, J. G. *et al.* The pathogenicity of long versus short fiber samples of amosite asbestos administered to rats by inhalation and intraperitoneal injection. *Br. J. Exp. Pathol.* **67**, 415–430 (1986).
- Kagan, V. E. *et al.* Direct and indirect effects of single walled carbon nanotubes on RAW 264.7 macrophages: role of iron. *Toxicol. Lett.* **165**, 88–100 (2006).
- Kamp, D. W., Graceffa, P., Pryor, W. A. & Weitzman, S. A. The role of free radicals in asbestos-induced diseases. *Free Radic. Biol. Med.* **12**, 293–315 (1992).
- Ye, J. *et al.* Critical role of glass fiber length in TNF-alpha production and transcription factor activation in macrophages. *Am. J. Physiol.* **276**, 426–434 (1999).
- McNally, A. K. & Anderson, J. M. Interleukin-4 induces foreign body giant cells from human monocytes/macrophages. Differential lymphokine regulation of macrophage fusion leads to morphological variants of multinucleated giant cells. *Am. J. Pathol.* **147**, 1487–1499 (1995).
- Maynard, A. D. *et al.* Exposure to carbon nanotube material: aerosol release during the handling of unrefined single-walled carbon nanotube material. *J. Toxicol. Environ. Health A* **67**, 87–107 (2004).
- World Health Organization. *Determination of Airborne Fibre Number Concentrations: A Recommended Method by Phase Contrast Optical Microscopy* (World Health Organization, Geneva, 1997).

Acknowledgements

We gratefully acknowledge Mitsui & Co. for the provision of a multiwalled carbon nanotube sample used. We thank S. Mitchell (University of Edinburgh) for sample preparation for SEM and technical assistance with the TEM and S. Clark (Institute of Occupational Medicine) for his technical assistance with the SEM. We thank the Colt Foundation (C.A.P., R.D., V.S. and K.D.), the Engineering and Physical Sciences Research Council (EPSRC) and the Royal Academy of Engineering (I.K.) for financial support.

Author contributions

C.A.P., R.D. and K.D. initiated, designed, directed and performed all experiments and took responsibility for planning and writing the manuscript. I.K. manufactured and provided the MWNT sample, NT_{long2}, and provided specialist input regarding CNT production and morphology. W.A.H.W. aided in the interpretation of the histological sections and contributed to the writing of the manuscript. A.M., A.S., S.B., V.S. and W.MacN. provided intellectual input and contributed to the writing of the manuscript.

Author information

Reprints and permission information is available online at <http://npj.nature.com/reprintsandpermissions/>. Correspondence and requests for materials should be addressed to K.D.